

# Thermal Stabilization of Proteins by Mono- and Oligosaccharides: Measurement and Analysis in the Context of an Excluded Volume Model

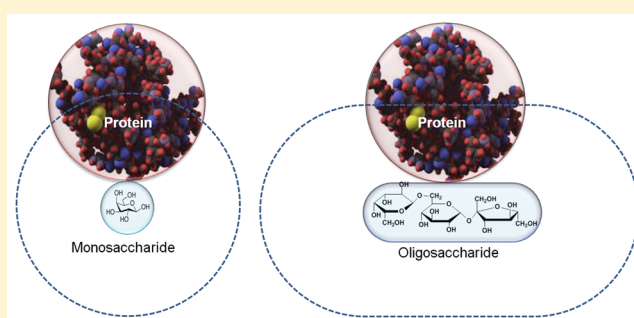
Ilyas Beg,<sup>†</sup> Allen P. Minton,<sup>\*,‡</sup> Md. Imtaiyaz Hassan,<sup>†</sup> Asimul Islam,<sup>†</sup> and Faizan Ahmad<sup>\*,†</sup>

<sup>†</sup>Centre for Interdisciplinary Research in Basic Sciences, Jamia Millia Islamia, Jamia Nagar, New Delhi 110025, India

<sup>‡</sup>National Institute of Diabetes and Digestive and Kidney Diseases, National Institutes of Health, Bethesda, Maryland 20892, United States

## S Supporting Information

**ABSTRACT:** The reversible thermal denaturation of apo  $\alpha$ -lactalbumin and lysozyme was monitored via measurement of changes in absorbance and ellipticity in the presence of varying concentrations of seven mono- and oligosaccharides: glucose, galactose, fructose, sucrose, trehalose, raffinose, and stachyose. The temperature dependence of the unfolding curves was quantitatively accounted for by a two-state model, according to which the free energy of unfolding is increased by an amount that is independent of temperature and depends linearly upon the concentration of added saccharide. The increment of added unfolding free energy per mole of added saccharide was found to depend approximately linearly upon the extent of oligomerization of the saccharide. The relative strength of stabilization of different saccharide oligomers could be accounted for by a simplified statistical–thermodynamic model attributing the stabilization effect to volume exclusion deriving from steric repulsion between protein and saccharide molecules.



Over the course of its lifetime, an organism may experience significant variation in environmental parameters such as temperature, pressure, salinity, and pH. A change in any of these variables is known to affect the functional properties of biological macromolecules and could in principle interfere with or inhibit essential processes necessary for the sustenance of life.<sup>1–4</sup> The process of evolution has therefore resulted in a variety of strategies for the protection of macromolecules from deleterious effects arising from environmental stress. One of these strategies is the accumulation of small organic molecules termed osmolytes<sup>5–9</sup> within cells and in extracellular fluids. *In vitro* experiments have shown that these molecules provide increased stability to proteins and other cell components against various stress conditions and maintain the normal functioning of the organism.<sup>6,10,11</sup> Chemically, osmolytes are classified into (i) amino acids and their derivatives, (ii) methylamines, and (iii) sugars and polyols.<sup>6,12</sup>

The mechanism underlying the stabilization of proteins by osmolytes has been the subject of extensive study.<sup>10,13–25</sup> On the basis of measurements of the free energy of transferring amino acid side chains and the peptide backbone from water to an osmolyte solution, Bolen and co-workers proposed a generalized physicochemical mechanism for the stabilization of proteins by osmolytes termed the “osmophobic effect”.<sup>19–24</sup> This effect derives from a highly unfavorable interaction of osmolytes with peptide backbone. Because unfolding of the protein results in an increased level of exposure of the

backbone to solvent, the free energy of the denatured state is increased relative to that of the native state, shifting the equilibrium between native and denatured states toward the native state.

In 1981, Lee and Timasheff<sup>26</sup> reported the first quantitative study of the thermal stabilization of three proteins,  $\alpha$ -chymotrypsin, chymotrypsinogen, and ribonuclease, by a saccharide, sucrose. Each of the proteins appeared to behave in accordance with a model in which the protein exists as a mixture of two thermodynamic states, native and unfolded, in dynamic equilibrium. The temperature at which each protein was observed to be half-folded, i.e., at which the equilibrium constant for unfolding was equal to unity, was observed to increase linearly with sucrose concentration. A van’t Hoff analysis of the temperature dependence of the equilibrium constant for unfolding at different sucrose concentrations indicated that sucrose did not significantly alter the enthalpy change accompanying unfolding of any of the three proteins; i.e., within experimental precision, the change in stability was due entirely to a decrease in the entropy change associated with unfolding. Careful measurement of the dependence of the partial specific volume of protein upon sucrose concentration

Received: April 17, 2015

Revised: May 21, 2015

Published: May 22, 2015

indicated that the concentration of sugar in the solvent immediately adjacent to the surface of each protein was lower than that in bulk solution (far from protein), in qualitative agreement with the osmophobic hypothesis. The authors concluded that the source of the stabilizing effect was a sugar-induced increase in the surface tension of the water/sugar solvent, i.e., the free energy of creating an interface between the sugar/water solution and any nonattracting medium, including the surface of a protein molecule. Because the unfolding of a globular protein is associated with an increase in solvent-accessible surface area, the free energy of unfolding is increased, shifting the equilibrium between native and unfolded states toward the native state.

More recently, Pielak, Erie, and co-workers characterized the effect of mono- and oligosaccharides on the stability of ferricytochrome *c* with respect to denaturation by temperature or by acidification at a constant temperature.<sup>10,11</sup> They reported that the increase in the free energy of two-state unfolding ( $\Delta\Delta G_{\text{NU}}$ ) in the presence of saccharide was proportional to the molar concentration of saccharide, and that the derivative of the free energy change with respect to sugar concentration ( $d\Delta\Delta G_{\text{NU}}/d[\text{saccharide}]$ ) was similar for two monosaccharides, similar and larger by a factor of  $\sim 2$  for two disaccharides, and slightly larger for a trisaccharide. They proposed that the observed phenomena could be qualitatively or semiquantitatively ascribed to a combination of a repulsive excluded volume interaction between protein and saccharide and a partially compensating weakly attractive chemical interaction. Most recently, O'Connor et al.<sup>27,28</sup> studied the effect of sucrose and fructose on the thermal stability of ribonuclease A and  $\alpha$ -lactalbumin and reported that the stabilization of both proteins by both sugars could be quantitatively accounted for by a simple excluded volume model.

This work was undertaken to further explore the stabilization of proteins by saccharides and to ascertain in greater detail the extent to which the magnitude of the stabilizing effect depends upon the chemical composition, size, and shape of the saccharide. Our results are qualitatively consistent with the results of prior investigations and support the general nature of the concept of osmophobicity. We demonstrate that the stabilizing effects of seven mono- and oligosaccharides upon two proteins may be accounted for quantitatively by a simple model with a very small number of adjustable parameters, based upon the assumption that the only significant interactions between all of the saccharides studied and both proteins are excluded volume interactions deriving from steric repulsion.

The statistical-thermodynamic formulation of the effect of volume exclusion upon chemical equilibria in the presence of a high concentration of chemically inert background molecules termed crowders has been summarized by Minton.<sup>29</sup> Over and above the qualitative prediction that volume exclusion by macromolecular crowders is expected to penalize the formation of the added solvent-accessible surface area associated with unfolding, the statistical-thermodynamic treatment makes specific predictions regarding the dependence of the magnitude of the stabilizing effect upon the size and shape of cosolute relative to that of the protein. To apply this formalism to the analysis of the effect of small molecule crowders in addition to macromolecular crowders, a semiempirical modification of the theory is proposed to allow for the diminution of the excluded volume effect as the size of a crowder molecule becomes smaller and approaches that of solvent molecules.

## MATERIALS AND METHODS

**Materials.** Commercially lyophilized hen egg white lysozyme and bovine  $\alpha$ -lactalbumin, sodium cacodylate trihydrate, and all sugars used in this study were purchased from Sigma Chemical Co. and used without further purification. Guanidinium chloride (GdmCl) was the ultrapure sample from MP Biomedical. All chemicals and reagents used were of analytical grade.

Lysozyme and holo  $\alpha$ -lactalbumin were dialyzed extensively against 0.1 M KCl, at pH 7.0. The apo form of  $\alpha$ -lactalbumin ( $\alpha$ -LA) was prepared by adding 5 mM EGTA to the solution of holo  $\alpha$ -lactalbumin during dialysis. Protein stock solutions were filtered using a 0.22  $\mu\text{M}$  Millipore syringe filter. Concentrations of lysozyme and  $\alpha$ -LA were determined experimentally using molar absorbance coefficient ( $\epsilon$ ) values of 39000  $\text{M}^{-1} \text{cm}^{-1}$  for lysozyme<sup>30</sup> and 29210  $\text{M}^{-1} \text{cm}^{-1}$  for  $\alpha$ -LA<sup>31</sup> at 280 nm. Concentrations of sugars (glucose, fructose, and sucrose)<sup>32</sup> and GdmCl<sup>33</sup> stock solutions were determined by refractive index measurements. However, concentrations of galactose, trehalose, raffinose, and stachyose were determined by dissolving a known amount of the respective sugar in the buffer. All measurements were taken in the degassed 0.05 M sodium cacodylate buffer containing 0.1 M KCl (pH 7.0). Because of the high stability of lysozyme in this buffer, we could not acquire an entire denaturation curve within the range of accessible temperatures. Lysozyme was therefore destabilized by addition of 2 M GdmCl to the buffer to allow an entire thermal denaturation curve to be measured within the range of accessible temperatures.

**Experimental Methods.** Absorption measurements were taken in a Jasco V-660 UV/vis spectrophotometer equipped with a Peltier-type temperature controller (ETCS-761). Thermal denaturations of  $\alpha$ -LA and lysozyme were monitored by following changes in  $\epsilon$  at 295 and 300 nm, respectively. The change in absorbance was monitored as a function of temperature in the range from 20 to 85  $^{\circ}\text{C}$  with a heating rate of 1  $^{\circ}\text{C min}^{-1}$ , an appropriate heating rate for providing adequate time for equilibration. Protein concentrations used for absorbance measurements were 0.4 and 0.5  $\text{mg mL}^{-1}$  for  $\alpha$ -LA and lysozyme, respectively. The raw absorbance data for each sample were converted into the change in molar extinction coefficient ( $\Delta\epsilon$ ,  $\text{M}^{-1} \text{cm}^{-1}$ ) at a given wavelength  $\lambda$ , where  $\Delta\epsilon(T) = \epsilon(T) - \epsilon(20^{\circ}\text{C})$ .

Because fructose used in our experiments absorbed in the near-UV region, the thermal denaturation of  $\alpha$ -LA and lysozyme in the presence of fructose could not be monitored by absorption measurements in the near-UV region. Denaturation in the presence of fructose was, therefore, followed by changes in ellipticity at 222 nm, as measured in a Jasco J-715 spectropolarimeter equipped with a Peltier-type temperature controller (PTC-348 WI). Thermal denaturation curves of both proteins in fructose are thus presented as plots of the CD signal at 222 nm as a function of temperature in the range of 20–85  $^{\circ}\text{C}$ . It should be noted that protein samples were heated at a rate of 1  $^{\circ}\text{C min}^{-1}$ . The protein concentration used for CD measurement was 0.3  $\text{mg mL}^{-1}$ . The raw CD data were expressed in terms of mean residue ellipticity  $[\theta]_{\lambda}$  (degrees per square centimeter per decimole) at a given wavelength  $\lambda$  using the relation

$$[\theta]_{\lambda} = (\theta_{\lambda} M_0) / (10lc) \quad (1)$$

where  $\theta_{\lambda}$  is the observed ellipticity in millidegrees at wavelength  $\lambda$ ,  $M_0$  is the mean residue weight of the protein,  $c$  is the protein

concentration in milligrams per milliliter, and  $l$  is the path length in centimeters.

The reversibility of thermal denaturation was ascertained by cooling the heated solution of denatured protein to 25 °C and comparing its optical signal to that of the protein prior to heating (Supporting Information Figure 1).

## DATA ANALYSIS

**Two-State Model for the Dependence of the Spectroscopic Signal upon Temperature in the Presence of Varying Concentrations of a Cosolute.** It is assumed that under the conditions used in our experiments, the reversible thermal denaturation of  $\alpha$ -LA and lysozyme in the absence of added sugar may be described by a two-state mechanism:



where  $N$  and  $U$  denote the native and unfolded states of proteins, respectively, and  $K_U^0(T)$  is the equilibrium constant for unfolding at temperature  $T$ , given by

$$K_U^0(T) = \exp[-\Delta G_U^0(T)/RT] \quad (3)$$

where  $R$  is the molar gas constant, and the temperature dependence of the free energy of unfolding ( $\Delta G_U^0$ ) is given by the Gibbs–Helmholtz relation:<sup>34</sup>

$$\Delta G_U^0(T) = \Delta H_{T_m}^0(1 - T/T_m^0) - \Delta C_p[(T_m^0 - T) + T \ln(T/T_m^0)] \quad (4)$$

where  $T$  denotes the absolute temperature,  $\Delta G_U^0$  is the temperature-dependent free energy change accompanying unfolding in the absence of added sugar,  $T_m^0$  is the temperature at which the protein is half-unfolded in the absence of sugar,  $\Delta H_{T_m}^0$  denotes the enthalpy change at  $T_m^0$ , and  $\Delta C_p$  is the heat capacity change accompanying unfolding, which is assumed to be independent of temperature. Equations 2–4 have been applied to previous studies of reversible two-state thermal unfolding.<sup>35–38</sup>

According to first-order excluded volume theory,<sup>29</sup> the effect of adding sugar is given by

$$\ln K_U(T) = \ln K_U^0(T) + \alpha c_s \quad (5)$$

where  $c_s$  is the concentration of sugar and the parameter  $\alpha$  is a temperature-independent function of the sizes and shapes of the protein and sugar, the molecular interpretation of which will be described subsequently. It follows from eqs 2–5 that the dependence of the fraction of unfolded protein ( $f_U$ ) upon temperature and sugar concentration is given by

$$f_U(T, c_s) = \frac{K_U(T)}{1 + K_U(T)} = \frac{\exp[\ln K_U^0(T) + \alpha c_s]}{1 + \exp[\ln K_U^0(T) + \alpha c_s]} \quad (6)$$

The change in any measurable property  $S$  of a protein undergoing a two-state transition from  $N$  to  $U$  is then given as a function of temperature by

$$S(T) = (1 - f_U)S_N(T) + f_U S_U(T) \quad (7)$$

where  $S_N(T)$  and  $S_U(T)$  denote the temperature-dependent properties of the  $N$  and  $U$  states, respectively. In our experiments, the signal  $S$  is an optical property (either absorbance or ellipticity) at a specific wavelength, measured

as a function of temperature in the absence and presence of various concentrations of different sugars. The dependence of  $S_N$  and  $S_U$  upon temperature at a specific wavelength  $\lambda$  is described by the empirical function<sup>39</sup>

$$S_N(T, \lambda) = a_1(\lambda) + a_2(\lambda)T_C + a_3(\lambda)T_C^2 \quad (8a)$$

$$S_U(T, \lambda) = a_4(\lambda) + a_5(\lambda)T_C + a_6(\lambda)T_C^2 \quad (8b)$$

where  $T_C$  denotes the temperature in degrees Celsius ( $T = T_C + 273.15$ ).

## Equivalent Hard Particle Model for the Dependence of $\alpha$ upon the Degree of Oligomerization of Saccharide.

The following is a highly simplified structural model based upon excluded volume theory that attempts to account for the dependency of stabilization parameter  $\alpha$  upon a particular protein–sugar pair in terms of the relative size and shape of each. The thermodynamic equilibrium constant for two-state unfolding is given by

$$K_U^0 = \frac{a_U}{a_N} = \frac{\gamma_U c_U}{\gamma_N c_N} \quad (9)$$

where  $a_X$ ,  $\gamma_X$ , and  $c_X$  denote the thermodynamic activity, thermodynamic activity coefficient, and molar concentration of species  $X$ , respectively. We can then define the experimentally accessible apparent equilibrium constant:

$$K_U \equiv \frac{c_U}{c_N} = K_U^0 \frac{\gamma_N}{\gamma_U} \quad (10)$$

which is equivalent to

$$\ln K_U = \ln K_U^0 + \ln \gamma_N - \ln \gamma_U \quad (11)$$

The logarithm of the activity coefficient of each solute species in the solution containing multiple solute species may be expanded in a power series of the concentration of all solutes:<sup>29</sup>

$$\ln \gamma_i = \sum_j B_{ij}c_j + \sum_j \sum_k B_{ijk}c_j c_k + \dots \quad (12)$$

$B_{ij}$  and  $B_{ijk}$  denote two- and three-body interaction coefficients, respectively. In this instance, the concentration of protein is so small that self-interaction between protein molecules may be neglected. In general, when the interaction between a macromolecule and small molecule is being assessed, three-body and higher-order interactions may be neglected, so that the small molecule has only a linear effect on the logarithm of the activity coefficient of the macromolecule. Thus, eq 12 reduces to the following expressions applying to the native and unfolded states of the protein in the presence of sugars:

$$\ln \gamma_N = B_{NS}c_s \quad (13a)$$

$$\ln \gamma_U = B_{US}c_s \quad (13b)$$

Equation 11 then reduces to

$$\ln K_U = \ln K_U^0 + (B_{NS} - B_{US})c_s \quad (14)$$

Comparison of eqs 5 and 14 leads to

$$\alpha = B_{NS} - B_{US} \quad (15)$$

Coefficients  $B_{NS}$  and  $B_{US}$  are thermodynamic parameters that are functions of the potential of mean force acting between a molecule of native protein and a molecule of sugar and between

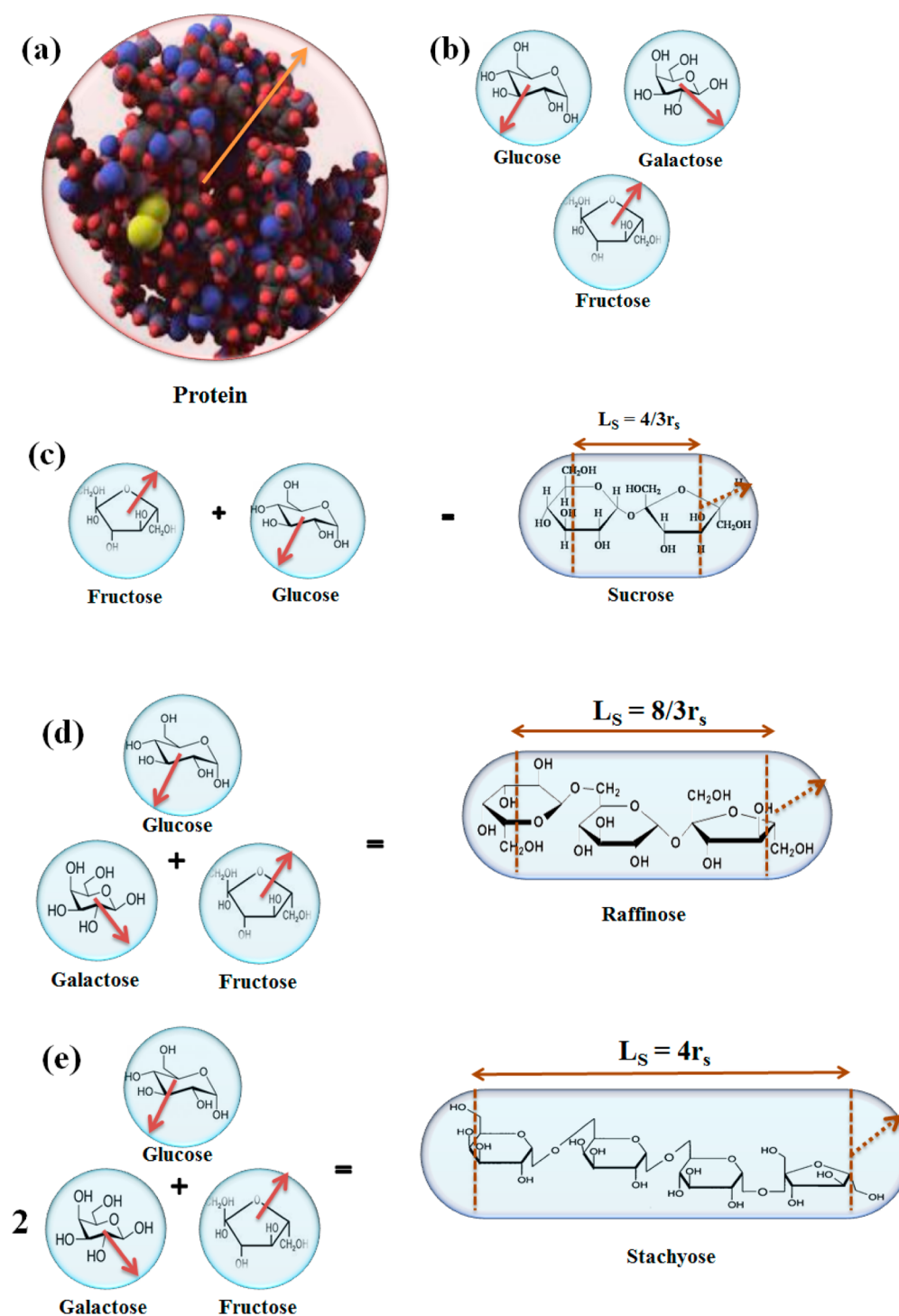


**Figure 1.** Representation of structural models. (a) The sphere represents the structure of the protein molecule containing the atomic structure of the protein. (b) Monosaccharides. Spheres represent the monosaccharides (glucose, galactose, and fructose), and each sphere contains the cyclic structure of the monosaccharide that exists in aqueous solution. (c) Disaccharides. Two units of monosaccharides constitute the disaccharide (glucose and fructose constitute sucrose), whereas in the case of trehalose, two molecules of glucose are covalently linked. (d) Trisaccharide. Raffinose, in which three monosaccharides (glucose, galactose, and fructose) are covalently linked. (e) Tetrasaccharide. Stachyose, in which four monosaccharide units (glucose, two galactoses, and fructose) are covalently linked. The full arrow in each sphere represents the radius of that sphere, and the dashed arrow in the spherocylinder represents the radius of the hemisphere.

a molecule of unfolded protein and a molecule of sugar, respectively.<sup>40</sup> In what follows, we attempt to approximate the potential of mean force by means of a simple structural model, according to which each molecule is represented by an equivalent hard convex particle that resembles the actual

molecule in size and shape. Hard particles are defined as impenetrable bodies that do not interact at distance greater than their contact distance. Equivalent hard particle models have proven to be useful in estimating the magnitude of nonspecific intermolecular interactions in a variety of macro-



molecular solutions.<sup>41</sup> By adopting an equivalent hard particle model, we achieve a great simplification, because in the case of interactions between hard particles:

$$B_{ij} = V_{ij} \quad (16)$$

where the quantity  $V_{ij}$ , called the co-volume of particles  $i$  and  $j$ , is the volume excluded by particle  $i$  to the center of mass of particle  $j$ , equal to the volume excluded by particle  $j$  to the center of mass of particle  $i$ .<sup>29</sup> We propose equivalent hard particle representations of all molecular species as follows.

**Native State of Proteins.**  $\alpha$ -LA and lysozyme are compact globular proteins of nearly identical size, crudely resembling prolate ellipsoids of rotation with an axial ratio of <2:1.<sup>42</sup> Their volumes ( $V$ , cubic centimeters per mole) are estimated according to

$$V = M\bar{v} \quad (17)$$

where  $M$  is the molar mass in grams per mole and  $\bar{v}$  is the partial specific volume in cubic centimeters per gram. For the purpose of estimating co-volumes, the native state of both proteins is represented by an equivalent sphere of equal volume, as indicated in Figure 1a.

**Unfolded "State" of Proteins.** From a theoretical point of view, this is the most difficult state to model as an equivalent hard particle, because we know that it exists as a manifold of conformations, and none of these conformations can be described as compact or globular.<sup>43,44</sup> The only assertion that can be made with confidence is that the radius of gyration of the unfolded protein is certain to be larger than that of the native protein. For the sake of simplicity, we shall model the unfolded state as an equivalent hard sphere with a radius given by

$$r_U = f_{\text{exp}} r_N \quad (18)$$

for example, a radius equal to that of the radius of the native state ( $r_N$ ) times an expansion factor  $f_{\text{exp}}$  that is >1. In fact, an expression mathematically equivalent to eq 18 may be derived from a more detailed treatment of the interaction of a hard particle crowder with an unfolded protein.<sup>44</sup> According to that treatment, the unfolded protein may be represented as a soft or porous sphere or, alternatively, a "cloud" of amino acid residues. The parameter  $f_{\text{exp}}$  is a function of the extent to which the hard particle crowder may penetrate into the element of volume occupied by the unfolded protein. As we have no way at present of estimating the value of this parameter *a priori*, it will be allowed to vary to achieve a best fit to the data.

**Mono- and Oligosaccharides.** The monosaccharides (glucose, galactose, and fructose) are represented by an equivalent sphere with a radius, denoted by  $r_s$ , equal to the hydrodynamic radius (i.e., 4 Å) calculated from measurements of diffusion.<sup>45</sup> Disaccharides (sucrose and trehalose), trisaccharides (raffinose), and tetrasaccharides (stachyose) are represented by an equivalent spherocylinder (a cylinder capped with two hemispheres) with a radius equal to  $r_s$ . The ratio of cylindrical length to diameter  $L_n$  of each oligosaccharide, where  $n$  denotes the degree of oligomerization, is calculated such that the volume of the spherocylinder representing the  $n$ -mer is equal to  $n$  times the volume of a monomer, for example

$$L_s = 4r_s(n - 1)/3 \quad (19)$$

Note that for  $n = 1$ , the equivalent spherocylinder reduces to the sphere as originally defined. Panels b and c of Figure 1 schematically depict the model structures of monosaccharides

(glucose, galactose, and fructose) and a disaccharide (sucrose), respectively, and panels d and e of Figure 1 depict the model structures of a trisaccharide (raffinose) and a tetrasaccharide (stachyose), respectively.

To examine whether it is important to take into account deviations from quasi-sphericity of oligosaccharides, a second simpler model for oligosaccharides was also formulated. According to this model, each oligosaccharide is represented by a spherical particle with a volume equal to  $n$  times the volume of the monosaccharide, i.e.,  $r_s(n) = n^{1/3}r_s(1)$  and  $L_s(n) = 0$ .

The co-volumes of the native or unfolded protein and each saccharide are calculated by observing that the co-volume  $V_{ij}$  of a sphere or spherocylinder representing species  $i$  and a sphere representing species  $j$  is the volume of a virtual particle that has the shape of species  $i$  but whose radius in all directions has been incremented by the radius of species  $j$ , as shown schematically in panels a and b of Figure 2, leading to

$$V_{NS} = 4\pi(r_N + r_s)^3/3 + \pi(r_N + r_s)^2L_s \quad (20a)$$

$$V_{US} = 4\pi(r_U + r_s)^3/3 + \pi(r_U + r_s)^2L_s \quad (20b)$$

where  $V_{NS}$  and  $V_{US}$  denote the co-volume of the native state and a sugar molecule and the co-volume of the unfolded state and a sugar molecule, respectively. Combination of eqs 15 and 16 leads to the relation

$$\alpha = V_{NS} - V_{US} \quad (21)$$

This expression would be correct if the reaction  $N \leftrightarrow U$  were taking place in the gas phase. However, the effect that we wish to model is the effect of a differential excluded volume in an aqueous solution. It is clear that the N and U states will exclude different volumes to the solvent (water) as well as the sugar. If one were to select a hypothetical crowder molecule that had roughly the same size and shape as a water molecule, the protein would exclude the same volume to both, and therefore, one would expect there to be no effect of the hypothetical small crowder on the unfolding equilibrium, which contradicts eq 21. Pielak and co-workers<sup>11</sup> attempted to address this difficulty by adopting an excluded volume model due to Berg,<sup>46</sup> in which the system is represented as a single large sphere representing protein (either N or U) and a variable concentration of smaller spheres representing saccharide within a dense fluid of even smaller spheres representing solvent (liquid water). The treatment of liquid water as a dense hard sphere fluid is highly questionable because of the neglect of strong hydrogen bonding interactions between water molecules. Hence, we adopt a simpler approximate correction that makes no assumptions regarding water–water interactions. This correction is based upon the observation, noted above, that a cosolute molecule having the same co-volume with protein as a water molecule should have no effect due to differential volume exclusion on the unfolding equilibria; i.e., for that "water-sized" cosolute,  $\alpha = 0$ . Equation 22 is therefore generalized to

$$\alpha = (V_{NS} - V_{US}) - (V_{NH} - V_{UH}) \quad (22)$$

where  $V_{NH}$  and  $V_{UH}$  denote the co-volumes of native and unfolded states and a water molecule, respectively. For the purpose of estimating  $V_{NH}$  and  $V_{UH}$ , we represent the water molecule by an equivalent hard sphere of radius  $r_H = 1.4$ – $1.6$  Å.<sup>47</sup> The co-volumes of N and U with water are then calculated according to

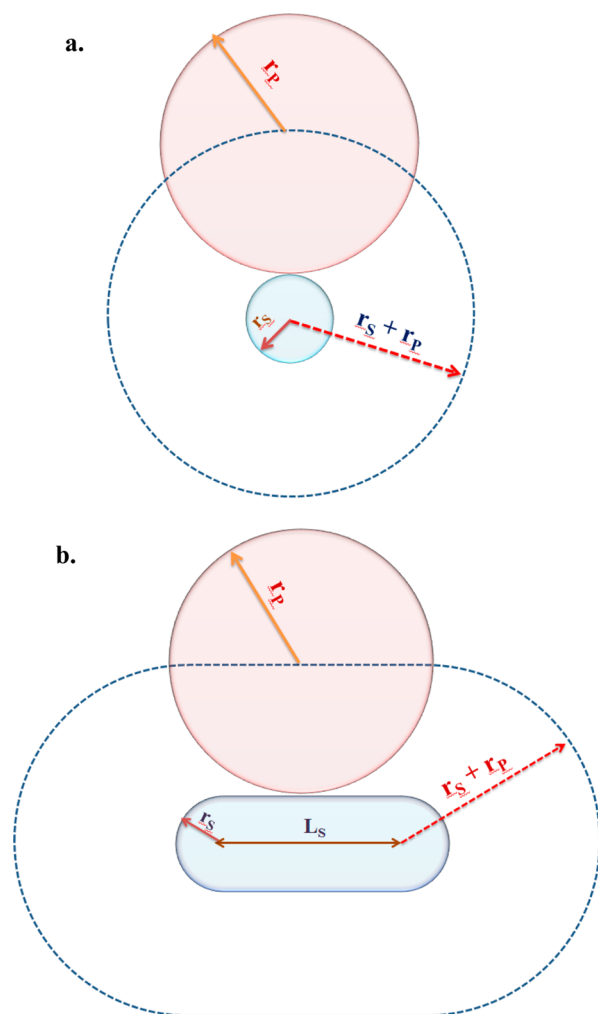


**Figure 2.** Representation of co-volumes of the protein and sugar molecules. (a) Co-volume of the protein with radius  $r_p$  and a monosaccharide with radius  $r_s$  represented by a dashed line sphere with radius  $r_s + r_p$ . (b) Co-volume of the protein with radius  $r_p$  and an oligosaccharide, represented by a spherocylinder with radius  $r_s$  and length  $L_s$ , will be a larger spherocylinder (dashed line) with radius  $r_s + r_p$  and length  $L_s$ .

$$V_{NH} = 4\pi(r_N + r_H)^3/3 \quad (23a)$$

$$V_{UH} = 4\pi(r_U + r_H)^3/3 \quad (23b)$$

Given values of  $r_N$ ,  $r_S$ , and  $r_H$  in angstroms and the unitless parameter  $f_{exp}$ , eqs 18–20, 22, and 23 may be used to calculate the value of  $\alpha$  (in units of cubic angstroms per molecule) as a function of  $n$ , the degree of oligomerization of saccharide. Unit conversion leads to

$$\alpha \text{ (1/mol)} = 6.02 \times 10^{-4} \times \alpha \text{ (Å}^3/\text{molecule)} \quad (24)$$

## RESULTS

To measure the effect of different sizes of sugars on the thermodynamic stability of proteins, we conducted reversible thermal denaturations of apo  $\alpha$ -lactalbumin ( $\alpha$ -LA) and lysozyme in the presence of different concentrations of three monosaccharides (glucose, galactose, and fructose), two disaccharides (sucrose and trehalose), a trisaccharide (raffinose), and a tetrasaccharide (stachyose) at pH 7.0. As described

in Materials and Methods, the extent of denaturation as a function of temperature was monitored by following  $\Delta\epsilon_{295}$  with increasing temperature for  $\alpha$ -LA and  $\Delta\epsilon_{300}$  for lysozyme, in the absence and presence of all sugars except fructose. Thermal denaturation of both proteins in the presence of fructose was measured by monitoring the change in  $[\theta]_{222}$ . It was ascertained that all of the denaturations of  $\alpha$ -LA and lysozyme performed as described in Materials and Methods were reversible over the entire range of sugar concentrations by cooling the heated solutions to the initial temperature (25 °C) and remeasuring the optical signal (Figure S1 of the Supporting Information). The measured dependence of absorbance or ellipticity of  $\alpha$ -LA solutions upon temperature in the absence and presence of various concentrations of each saccharide is plotted in Figure 3A–G. Analogous data obtained from lysozyme solutions are plotted in Figure 4A–G.

The excluded volume model described in Materials and Methods (eqs 3–8) was fit to the combined dependence of the absorbance or ellipticity of each protein upon temperature, in the absence and presence of all concentrations of each sugar via nonlinear least-squares minimization to obtain best-fit values of the 10 adjustable parameters defined in the description of the model:  $T_m^0$ ,  $\Delta H_{T_m^0}$ ,  $\Delta C_p$ ,  $a_1$ – $a_6$ , and  $\alpha$ . The best-fit values of  $T_m^0$ ,  $\Delta H_{T_m^0}$ , and  $\Delta C_p$  obtained from the thermal denaturations of  $\alpha$ -LA and lysozyme at pH 7.0 under our experimental conditions are listed in Table 1. The indicated uncertainties in  $T_m^0$ ,  $\Delta H_{T_m^0}$ , and  $\Delta C_p$  correspond to one standard error of the estimate. Denaturation curves calculated using eqs 3–8 with the best-fit values of all adjustable parameters are plotted together with the data in Figures 3 and 4. The best-fit value of  $\alpha$  obtained for each protein–sugar pair is given in Table 2 and plotted as a function of the degree of oligomerization of the saccharide in Figure 5. Indicated uncertainties in the measurement of  $\alpha$  correspond to  $\pm 2$  standard errors of the estimate (i.e., 95% confidence limits).

The structural model for the dependence of  $\alpha$  for each protein–sugar pair on the degree of oligomerization described in Materials and Methods (eqs 15–23) was fitted to the data for each protein plotted in Figure 5, allowing only the value of parameter  $f_{exp}$  to vary to minimize the sum of squared residuals. The dependence calculated using the best-fit values of  $f_{exp}$  for each protein given in the figure caption is plotted together with the data in Figure 5. The solid line is the best fit of the version of the model in which oligosaccharides are represented as equivalent spherocylinders, and the dashed line is the best fit of the version in which oligosaccharides are represented as equivalent spheres. While the data obtained from lysozyme solutions are described roughly equally well by both representations of oligosaccharide, the data obtained from the  $\alpha$ -LA solutions seem to be significantly better described by the version of the model in which oligosaccharides are represented by spherocylinders.

## DISCUSSION

The two-state model for the dependence of the spectroscopic signal on temperature presented here is based upon the following assumptions. (1)  $T_m^0$ ,  $\Delta H_{T_m^0}$ , and  $\Delta C_p$  are assumed to be common to all data sets obtained for a particular protein under the conditions of our experiments, described in Materials and Methods, because they are properties of that protein in the experimental buffer in the absence of sugar. (2) The  $a_i$  values

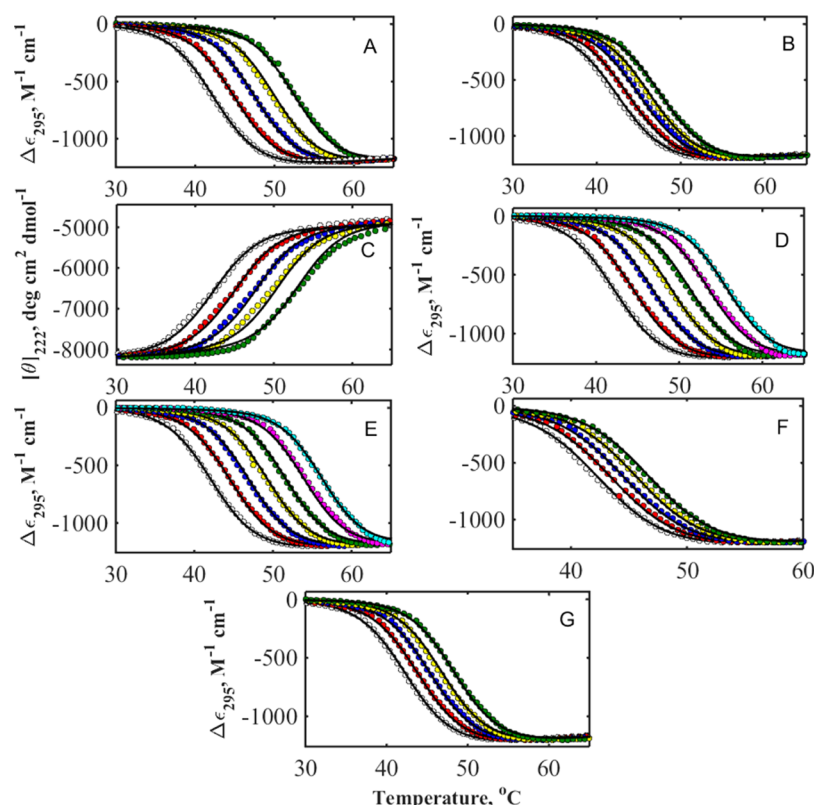


**Figure 3.** Representative curves of thermal denaturations of  $\alpha$ -LA in the absence and presence of different concentrations of mono- and oligosaccharides at pH 7.0. Data sets in each panel from left to right correspond to incrementally increasing molar concentrations of saccharide denoted by the notation  $a:b:c$ , where  $a$  is the lowest molar concentration,  $b$  the increment, and  $c$  the highest concentration of saccharide: (A) glucose 0:0.5:2.0, (B) galactose 0:0.25:1.0, (C) fructose 0:0.5:2.0, (D) sucrose 0:0.25:1.5, (E) trehalose 0:0.25:1.5, (F) raffinose 0:0.1:0.4, and (G) stachyose 0:0.1:0.4. Solid curves are plotted according to eqs 3–8 using the values of  $\alpha$  for each saccharide plotted in Figure 5. Although all denaturation curves were measured in the temperature range of 20–85 °C, for the sake of clarity, some denaturation curves are shown over expanded temperature ranges.

are assumed to depend only upon the property measured (absorbance or ellipticity) and to be independent of sugar composition or concentration. (3) The effect of each sugar on the stability of each protein is quantified by the single temperature-independent parameter  $\alpha$  defined in eq 5. Using this model, we can describe all denaturation curves obtained for an individual protein in multiple concentrations of multiple saccharides within experimental uncertainty with only 22 adjustable parameters ( $T_m^0$ ,  $\Delta H_{T_m^0}^0$ ,  $\Delta C_p$ , two sets of  $a_1$ – $a_6$  for absorbance and ellipticity measurements, and one value of  $\alpha$  for each saccharide). This is to be contrasted with the conventional description of individual two-state thermal denaturation curves,<sup>36,39,48–50</sup> which requires seven to nine adjustable parameters per curve, or at least 238 adjustable parameters for all 34 data sets obtained from  $\alpha$ -LA solutions, and an equal number for all data obtained from lysozyme solutions.

The success of this model in providing an accurate yet extremely parsimonious description of the data argues for the validity of the assumption that the addition of a saccharide to either of the proteins examined stabilizes that protein by decreasing the entropy change associated with unfolding without significantly affecting the enthalpy change.

The plot of best-fit values of  $\alpha$  versus  $n$ , the degree of saccharide oligomerization (Figure 5), indicates that the value of  $\alpha$  is insensitive to the sequence of saccharide subunits in an oligomer and depends approximately linearly upon the degree of saccharide oligomerization up to  $n = 4$ .

The equivalent hard particle model for excluded volume interaction between saccharide and protein was found to provide a reasonably accurate description of the dependence of  $\alpha$  upon  $n$  for each protein, with only a single adjustable parameter for each protein,  $f_{\text{exp}}$ . The representation of the oligosaccharide as an equivalent spherocylinder seems to model the data slightly better than the representation of oligosaccharide as an equivalent sphere, although these structural models are as a whole so approximate that the difference may not be significant. Interestingly, the best-fit values of  $f_{\text{exp}}$  are smaller than one might expect for a fully unfolded random coil protein and probably indicate that the four sulfhydryl cross-links in each protein greatly reduce the extent of expansion accompanying thermal unfolding, as suggested by Goldenberg.<sup>51</sup>

While the simplifying assumptions upon which these models are based are evident, we believe that they do not render invalid the derived conclusions. The assumption that the interaction between saccharides and these proteins is essentially entirely due to excluded volume (i.e., an entropic effect) is consistent not only with the data reported here but also with the earlier finding<sup>26</sup> that added sucrose stabilized  $\alpha$ -chymotrypsin, chymotrypsinogen, and ribonuclease against thermal unfolding without significantly altering the enthalpy change associated with unfolding of any of the three proteins. The use of equivalent hard particle models to estimate the energetic consequences of excluded volume interactions has provided

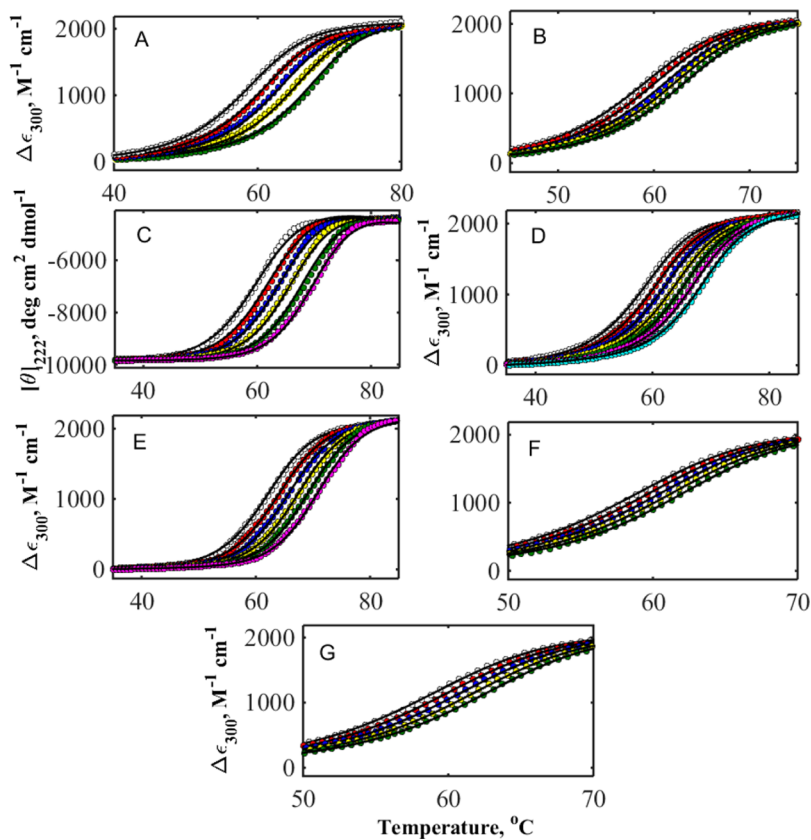


**Figure 4.** Representative curves of thermal denaturations of lysozyme in the absence and presence of different concentrations of mono- and oligosaccharides at pH 7.0. The panels correspond to the same saccharides and concentration ranges as in Figure 3. (In panel E, the data set corresponding to no added saccharide was deleted as a statistically significant outlier indicating systematic error of measurement.) Solid curves are plotted according to eqs 3–8 with best-fit values of  $\alpha$  for each saccharide plotted in Figure 5. Although all denaturation curves were measured in the temperature range of 20–85 °C, for the sake of clarity, some denaturation curves are shown over expanded temperature ranges. Thermal denaturations of lysozyme were conducted in the presence of 2 M GdmCl (the reason for the addition of 2 M GdmCl is given in Materials and Methods).

**Table 1. Thermodynamic Parameters Obtained from Thermal Denaturations of  $\alpha$ -LA and Lysozyme in the Absence of Sugar at pH 7.0<sup>a</sup>**

protein	$T_m^0$ (°C)	$\Delta H_m^0$ (kcal mol <sup>-1</sup> )	$\Delta C_p$ (cal mol <sup>-1</sup> K <sup>-1</sup> )
$\alpha$ -LA	42.3 ± 0.04	69.2 ± 0.30	830 ± 14
lysozyme <sup>b</sup>	59.4 ± 0.20	51.4 ± 0.61	1035 ± 60

<sup>a</sup>Indicated uncertainties correspond to ±1 standard error of the mean.

<sup>b</sup>Thermodynamic parameters of lysozyme in the presence of 2 M GdmCl (for details, see the text).

**Table 2. Values of Stabilization Parameter  $\alpha$  for  $\alpha$ -LA and Lysozyme in the Presence of Different Sugars at pH 7.0<sup>a</sup>**

sugar	$-\alpha$ (L mol <sup>-1</sup> ) <sup>b</sup>	
	$\alpha$ -LA	lysozyme
glucose	1.85 ± 0.20	1.03 ± 0.26
galactose	1.80 ± 0.30	0.99 ± 0.20
fructose	1.45 ± 0.20	1.06 ± 0.30
sucrose	3.28 ± 0.30	1.49 ± 0.20
trehalose	3.43 ± 0.30	1.74 ± 0.30
raffinose	3.75 ± 0.80	1.81 ± 0.36
stachyose	5.25 ± 1.00	2.17 ± 0.40

<sup>a</sup>Indicated uncertainties correspond to ±2 standard errors of the estimate (95% confidence limits). <sup>b</sup>The negative sign indicates the exclusion of saccharide from the protein surface.

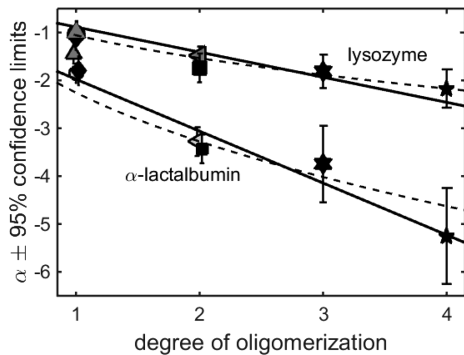


**Figure 5.** Plot of the dependence of stabilization factor  $\alpha$  upon the degree of oligomerization ( $n$ ) of  $\alpha$ -LA and lysozyme: (circles) glucose, (triangles) fructose, (diamonds) galactose, (empty triangles) sucrose, (squares) trehalose, (hexagons) raffinose, and (pentagons) stachyose. Curves are best fits of equivalent hard particle models described in the text. Solid lines are best fits of the model with saccharides represented by equivalent hard spherocylinders, calculated using best-fit values of  $f_{\text{exp}}$  for  $\alpha$ -LA and lysozyme equal to  $1.16 \pm 0.01$  and  $1.07 \pm 0.015$ , respectively. Indicated uncertainties represent 95% confidence intervals. Dashed lines are best fits of the model with saccharides represented by equivalent hard spheres, calculated using best-fit values of  $f_{\text{exp}}$  for  $\alpha$ -LA and lysozyme equal to 1.17 and 1.09, respectively.

physically reasonable quantitative and semiquantitative interpretations of the dependence of many experimentally observed



solution properties upon the composition dependence of these solutions.<sup>29,52,53</sup> The ability of these models, and the models presented here in particular, to account quantitatively for large bodies of data in a parsimonious fashion provides strong evidence that an atomistic representation of molecules is not required to obtain reasonably accurate estimates of the magnitude of excluded volume interactions between them.

## ■ ASSOCIATED CONTENT

### ■ Supporting Information

Spectra of  $\alpha$ -LA and lysozyme at pH 7.0. The Supporting Information is available free of charge on the ACS Publications website at DOI: 10.1021/acs.biochem.5b00415.

## ■ AUTHOR INFORMATION

### Corresponding Authors

\*Centre for Interdisciplinary Research in Basic Sciences, Jamia Millia Islamia, New Delhi 110025, India. Telephone: 91-11-26321733. Fax: 91-11-26983409. E-mail: fahmad@jmi.ac.in.

\*National Institute of Diabetes and Digestive and Kidney Diseases, National Institutes of Health, Bethesda, MD 20892. E-mail: minton@helix.nih.gov.

### Funding

The research of F.A. and A.I. was supported by the Council of Scientific and Industrial Research, India [Grants 37(1603)/13/EMRII and 37(1604)/13/EMRII]. The research of A.P.M. was supported by the Intramural Research Program of the National Institute of Diabetes and Digestive and Kidney Diseases.

### Notes

The authors declare no competing financial interest.

## ■ ACKNOWLEDGMENTS

We thank Professor Rajiv Bhat (Jawaharlal Nehru University, New Delhi, India) for helpful and constructive comments on a draft of this report. A.P.M. thanks the Jawaharlal Nehru Institute of Advanced Study (JNIAS) and Professors Ummu Salma Bava, Arun K. Attri, and Rajiv Bhat (Jawaharlal Nehru University) for hospitality extended during his tenure as a JNIAS Invited Fellow, from January to March 2014, during which period his participation in this research was initiated.

## ■ ABBREVIATIONS

$\alpha$ -LA, apo  $\alpha$ -lactalbumin; GdmCl, guanidinium chloride

## ■ REFERENCES

- (1) Jaenicke, R. (1991) Protein stability and molecular adaptation to extreme conditions. *Eur. J. Biochem.* 202, 715–728.
- (2) Jaenicke, R., and Bohm, G. (1998) The stability of proteins in extreme environments. *Curr. Opin. Struct. Biol.* 8, 738–748.
- (3) Krasensky, J., and Jonak, C. (2012) Drought, salt, and temperature stress-induced metabolic rearrangements and regulatory networks. *J. Exp. Bot.* 63, 1593–1608.
- (4) Arakawa, T., Prestrelski, S. J., Kenney, W. C., and Carpenter, J. F. (2001) Factors affecting short-term and long-term stabilities of proteins. *Adv. Drug Delivery Rev.* 46, 307–326.
- (5) Yancey, P. H., and Somero, G. N. (1979) Counteraction of urea destabilization of protein structure by methylamine osmoregulatory compounds of elasmobranch fishes. *Biochem. J.* 183, 317–323.
- (6) Yancey, P. H., Clark, M. E., Hand, S. C., Bowlus, R. D., and Somero, G. N. (1982) Living with water stress: Evolution of osmolyte systems. *Science* 217, 1214–1222.
- (7) Wang, A., and Bolen, D. W. (1997) A naturally occurring protective system in urea-rich cells: Mechanism of osmolyte protection of proteins against urea denaturation. *Biochemistry* 36, 9101–9108.

(8) Burg, M. B., and Peters, E. M. (1997) Urea and methylamines have similar effects on aldose reductase activity. *Am. J. Physiol.* 273, F1048–F1053.

(9) Santoro, M. M., Liu, Y., Khan, S. M., Hou, L. X., and Bolen, D. W. (1992) Increased thermal stability of proteins in the presence of naturally occurring osmolytes. *Biochemistry* 31, 5278–5283.

(10) Davis-Searles, P. R., Saunders, A. J., Erie, D. A., Winzor, D. J., and Pielak, G. J. (2001) Interpreting the effects of small uncharged solutes on protein-folding equilibria. *Annu. Rev. Biophys. Biomol. Struct.* 30, 271–306.

(11) Saunders, A. J., Davis-Searles, P. R., Allen, D. L., Pielak, G. J., and Erie, D. A. (2000) Osmolyte-induced changes in protein conformational equilibria. *Biopolymers* 53, 293–307.

(12) Jamal, S., Poddar, N. K., Singh, L. R., Dar, T. A., Rishi, V., and Ahmad, F. (2009) Relationship between functional activity and protein stability in the presence of all classes of stabilizing osmolytes. *FEBS J.* 276, 6024–6032.

(13) Arakawa, T., and Timasheff, S. N. (1982) Stabilization of protein structure by sugars. *Biochemistry* 21, 6536–6544.

(14) Timasheff, S. N. (2002) Protein-solvent preferential interactions, protein hydration, and the modulation of biochemical reactions by solvent components. *Proc. Natl. Acad. Sci. U.S.A.* 99, 9721–9726.

(15) Arakawa, T., and Timasheff, S. N. (1982) Preferential interactions of proteins with salts in concentrated solutions. *Biochemistry* 21, 6545–6552.

(16) Timasheff, S. N. (2002) Protein hydration, thermodynamic binding, and preferential hydration. *Biochemistry* 41, 13473–13482.

(17) Timasheff, S. N. (1993) The control of protein stability and association by weak interactions with water: How do solvents affect these processes? *Annu. Rev. Biophys. Biomol. Struct.* 22, 67–97.

(18) Xie, G., and Timasheff, S. N. (1997) Mechanism of the stabilization of ribonuclease A by sorbitol: Preferential hydration is greater for the denatured than for the native protein. *Protein Sci.* 6, 211–221.

(19) Bolen, D. W., and Baskakov, I. V. (2001) The osmophobic effect: Natural selection of a thermodynamic force in protein folding. *J. Mol. Biol.* 310, 955–963.

(20) Liu, Y., and Bolen, D. W. (1995) The peptide backbone plays a dominant role in protein stabilization by naturally occurring osmolytes. *Biochemistry* 34, 12884–12891.

(21) Baskakov, I., and Bolen, D. W. (1998) Forcing thermodynamically unfolded proteins to fold. *J. Biol. Chem.* 273, 4831–4834.

(22) Qu, Y., Bolen, C. L., and Bolen, D. W. (1998) Osmolyte-driven contraction of a random coil protein. *Proc. Natl. Acad. Sci. U.S.A.* 95, 9268–9273.

(23) Bolen, D. W. (2001) Protein stabilization by naturally occurring osmolytes. *Methods Mol. Biol.* 168, 17–36.

(24) Auton, M., Rosgen, J., Sinev, M., Holthausen, L. M., and Bolen, D. W. (2011) Osmolyte effects on protein stability and solubility: A balancing act between backbone and side-chains. *Biophys. Chem.* 159, 90–99.

(25) Kaushik, J. K., and Bhat, R. (2003) Why is trehalose an exceptional protein stabilizer? An analysis of the thermal stability of proteins in the presence of the compatible osmolyte trehalose. *J. Biol. Chem.* 278, 26458–26465.

(26) Lee, J. C., and Timasheff, S. N. (1981) The stabilization of proteins by sucrose. *J. Biol. Chem.* 256, 7193–7201.

(27) O'Connor, T. F., DeBenedetti, P. G., and Carbeck, J. D. (2004) Simultaneous determination of structural and thermodynamic effects of carbohydrate solutes on the thermal stability of ribonuclease A. *J. Am. Chem. Soc.* 126, 11794–11795.

(28) O'Connor, T. F., DeBenedetti, P. G., and Carbeck, J. D. (2007) Stability of proteins in the presence of carbohydrates; experiments and modeling using scaled particle theory. *Biophys. Chem.* 127, 51–63.

(29) Minton, A. P. (1998) Molecular crowding: Analysis of effects of high concentrations of inert cosolutes on biochemical equilibria and rates in terms of volume exclusion. *Methods Enzymol.* 295, 127–149.

- (30) Hamaguchi, K., and Kurono, A. (1963) Structure of Muramidase (Lysozyme). I. The Effect of Guanidine Hydrochloride on Muramidase. *J. Biochem.* 54, 111–122.
- (31) Sugai, S., Yashiro, H., and Nitta, K. (1973) Equilibrium and kinetics of the unfolding of  $\alpha$ -lactalbumin by guanidine hydrochloride. *Biochim. Biophys. Acta* 328, 35–41.
- (32) Weast, R. C. (1972) *Handbook of Chemistry and Physics*, CRC Press, Cleveland, OH.
- (33) Pace, C. N. (1986) Determination and analysis of urea and guanidine hydrochloride denaturation curves. *Methods Enzymol.* 131, 266–280.
- (34) Becktel, W. J., and Schellman, J. A. (1987) Protein stability curves. *Biopolymers* 26, 1859–1877.
- (35) Haque, I., Islam, A., Singh, R., Moosavi-Movahedi, A. A., and Ahmad, F. (2006) Stability of proteins in the presence of polyols estimated from their guanidinium chloride-induced transition curves at different pH values and 25 °C. *Biophys. Chem.* 119, 224–233.
- (36) Swint, L., and Robertson, A. D. (1993) Thermodynamics of unfolding for turkey ovomucoid third domain: Thermal and chemical denaturation. *Protein Sci.* 2, 2037–2049.
- (37) Khan, S., Bano, Z., Singh, L. R., Hassan, M. I., Islam, A., and Ahmad, F. (2013) Testing the ability of non-methylamine osmolytes present in kidney cells to counteract the deleterious effects of urea on structure, stability and function of proteins. *PLoS One* 8, e72533.
- (38) Haque, I., Singh, R., Ahmad, F., and Moosavi-Movahedi, A. A. (2005) Testing polyols' compatibility with Gibbs energy of stabilization of proteins under conditions in which they behave as compatible osmolytes. *FEBS Lett.* 579, 3891–3898.
- (39) Yadav, S., and Ahmad, F. (2000) A new method for the determination of stability parameters of proteins from their heat-induced denaturation curves. *Anal. Biochem.* 283, 207–213.
- (40) McMillan, W. G., and Mayer, J. E. (1945) The Statistical Thermodynamics of Multicomponent Systems. *J. Chem. Phys.* 13, 276–305.
- (41) Minton, A. P. (2007) The effective hard particle model provides a simple, robust, and broadly applicable description of nonideal behavior in concentrated solutions of bovine serum albumin and other nonassociating proteins. *J. Pharm. Sci.* 96, 3466–3469.
- (42) Lee, J. C., and Timasheff, S. N. (1974) Partial specific volumes and interactions with solvent components of proteins in guanidine hydrochloride. *Biochemistry* 13, 257–265.
- (43) Minton, A. P. (2001) Effects of excluded surface area and adsorbate clustering on surface adsorption of proteins. II. Kinetic models. *Biophys. J.* 80, 1641–1648.
- (44) Minton, A. P. (2005) Models for excluded volume interaction between an unfolded protein and rigid macromolecular cosolutes: Macromolecular crowding and protein stability revisited. *Biophys. J.* 88, 971–985.
- (45) Schultz, S. G., and Solomon, A. K. (1961) Determination of the effective hydrodynamic radii of small molecules by viscometry. *J. Gen. Physiol.* 44, 1189–1199.
- (46) Berg, O. G. (1990) The influence of macromolecular crowding on thermodynamic activity: Solubility and dimerization constants for spherical and dumbbell-shaped molecules in a hard-sphere mixture. *Biopolymers* 30, 1027–1037.
- (47) Lee, B., and Richards, F. M. (1971) The interpretation of protein structures: Estimation of static accessibility. *J. Mol. Biol.* 55, 379–400.
- (48) Wang, Y., Sarkar, M., Smith, A. E., Krois, A. S., and Pielak, G. J. (2012) Macromolecular crowding and protein stability. *J. Am. Chem. Soc.* 134, 16614–16618.
- (49) Sinha, A., Yadav, S., Ahmad, R., and Ahmad, F. (2000) A possible origin of differences between calorimetric and equilibrium estimates of stability parameters of proteins. *Biochem. J.* 345 (Part 3), 711–717.
- (50) Santoro, M. M., and Bolen, D. W. (1992) A test of the linear extrapolation of unfolding free energy changes over an extended denaturant concentration range. *Biochemistry* 31, 4901–4907.
- (51) Goldenberg, D. P. (2003) Computational simulation of the statistical properties of unfolded proteins. *J. Mol. Biol.* 326, 1615–1633.
- (52) Zimmerman, S. B., and Minton, A. P. (1993) Macromolecular crowding: Biochemical, biophysical, and physiological consequences. *Annu. Rev. Biophys. Biomol. Struct.* 22, 27–65.
- (53) Hall, D., and Minton, A. P. (2003) Macromolecular crowding: Qualitative and semiquantitative successes, quantitative challenges. *Biochim. Biophys. Acta* 1649, 127–139.